GEOPHYSICAL RESEARCH LETTERS, VOL. 25, NO.18, PAGES 3533-3536, SEPTEMBER 15, 1998

Sediment resuspension in the wakes of Hurricanes Edouard and Hortense

T. D. Dickey,[1] G. C. Chang,[1] Y. C. Agrawal,[2] A. J. Williams, III,[3] and P. S. Hill[4]

Abstract. A unique set of physical and optical observations of sediment resuspension was obtained during the passage of two hurricanes, Edouard and Hortense. The eyes of these hurricanes passed within approximately 110 and 350 km, respectively, of our study site on the continental shelf (100 km south of Cape Cod, Massachusetts) within a two-week period in the fall of 1996. Sediments were resuspended to more than 30 m above the ocean bottom during both hurricanes. The sediment resuspension processes associated with the two hurricanes are shown to differ primarily because of the separation distances between the eyes of the hurricanes and the observational site (e.g., local versus remote forcing). Observed particle-size distributions were shifted toward smaller scales during Hurricane Edouard because of flocculate disaggregation caused by high levels of localized shear and turbulence.

Introduction

The present report describes physical and optical measurements relevant to sediment resuspension on a continental shelf during the passage of two hurricanes within a two-week period. Our results are especially important as few observations of resuspension have been made under extreme atmospheric forcing (e.g., Madsen et al. [1993]). Such observations are of great interest as they enable the study of episodic processes that modify the near-bottom environment and control the fate of bottom materials including sediments, organisms, and pollutants that are transported, deposited, and transformed on continental shelves (e.g., Churchill [1989]; Cacchione and Drake [1990]; Nittrouer and Wright [1994]). Physical processes that can contribute to sediment resuspension and transport include wind-generated surface waves, internal gravity and solitary waves, tides, mean interior and boundary layer currents, eddies, and buoyancy-driven plumes (e.g., Cacchione and Drake [1990]; Nittrouer and Wright [1994]). Further, there is a complex interplay between physical, geological, and biological processes involving particles and organisms of varying size, shape, and buoyancy (e.g., Nowell [1983]). These processes result in a change in particle-size distributions. The present measurements provide insights into the dynamical processes that result in sediment resuspension during intense forcing and the relaxation to more normal near-bottom conditions, as well as variability in near-bottom particle-size distributions. These observations allow investigators to test model hypotheses and performance.

[1]Ocean Physics Laboratory, University of California at Santa Barbara, Santa Barbara, California.

[2]Sequoia Scientific, Inc., Mercer Island, Washington.

[3]Woods Hole Oceanographic Institution, Woods Hole, Massachusetts.

[4]Department of Oceanography, Dalhousie University, Halifax, Nova Scotia, Canada.

Paper number 98GL02635.
0094-8534/98/98GL-02635$05.00

The present site is located in a region known as the "Mud Patch" on the Mid-Atlantic Bight shelf off the east coast of the U.S. (Fig. 1) where extensive observations have been made in the past (e.g., Biscaye et al. [1988]). The Mud Patch is a deposit of 2 to 14 m thickness covering an area of roughly 100 km by 200 km composed of relatively uniform fine-grained material overlying coarser sand-sized sediment [Twichell et al., 1987]. The sediment consists primarily of fine-textured material.

Methods

The present experiment consisted of four deployments (spanning summer 1996 through summer 1997) of a mooring and two bottom tripods located at approximately 40.5°N, 70.5°W in waters of about 70 m depth (Fig. 1). The time series described here were obtained during the first deployment period.

Several physical and optical measurement systems were deployed on the mooring (Fig. 1). These included bio-optical systems (BIOPS) (as described in Chang et al. [1997]; Dickey et al. [1998]), which were placed at 14, 37, and 52 m depths to quantify optical and physical variability. A subset of BIOPS sensors used for this study included 1) ac-9s, 2) fluorometers, and 3) temperature sensors. The sampling rate for the ac-9 was once per hour for 30 seconds and the sampling rate for all other sensors was eight times per hour. Vector winds were measured from a nearby surface buoy with an anemometer at 3.3 m above the surface. In addition, wave data were measured by National Data Buoy Center (NDBC) buoy 44008, located at 40.5°N, 69.43°W (90 km east of the CMO site).

A nearby optical bottom tripod consisted of a suite of instruments designed to measure properties of particles (Fig. 1). The BIOPS, as described above, was mounted at 1.5 meters above the bottom (mab) (~68 m depth). A photographic camera was placed on the tripod at 1 mab and was used to measure size distributions of particles larger than 500 μm in the bottom boundary layer. The final set of instruments measured true volumetric concentration of fine particles derived from size distribution using the LISST-100 [Agrawal and Pottsmith, 1994]. The LISST-100, measuring the size distribution at 1.6 mab, was sampled at 15-minute intervals and on the hour.

The other bottom tripod (also located at a depth of 70 m and about 400 m from the mooring) was used to measure near-bottom currents. BASS current meters [Williams et al., 1987] recorded vector velocities at seven depths from 0.38 to 7 mab. These measurements were made on the hour and half-hour with sampling at 2 Hz for 28 min and 49 sec. Mean current bottom shear stress (τ_c), wave-orbital velocity (u_w), current-wave bottom shear stress (τ_{c+w}), and dissipation rate (ε_{c+w}) were computed using time series velocity data collected by the BASS current meters to characterize the near-bottom flow field responsible for sediment resuspension. Wave-orbital velocity was estimated by taking the square root of the integral of energy under the wave peak in the velocity spectra (periods from 8 to 25 s). Mean current bottom shear stress was computed from BASS current meter data and the "law of the wall" formulation [Tennekes and Lumley, 1972].

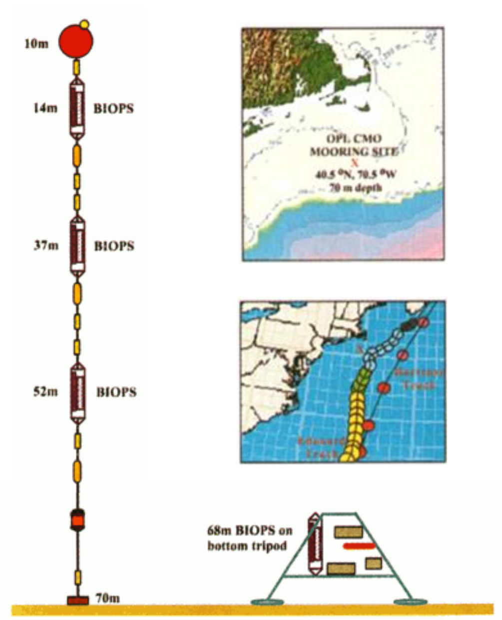

Figure 1. Geographic map indicating site of mooring and tripods used for the present study. Map showing tracks of Hurricanes Edouard and Hortense. Mooring and optical tripod schematic diagrams.

A number of models have been formulated to characterize near-bottom combined wave and current flow (e.g., Grant and Madsen [1979], and Christoffersen and Jonsson [1985]). More advanced versions of bottom boundary layer models that include effects of armoring, moveable beds, and/or stratified flows have been described by Trowbridge and Madsen [1984] and Glenn and Grant [1987]. These advanced versions were not used in the present study due to the absence of bottom sediment condition data and the presence of a well-mixed bottom boundary layer. The Christoffersen and Jonsson [1985] model was chosen to compute bottom shear stress from combined current and wave motion at 0.38 mab. The model is quite similar to the commonly used Grant and Madsen [1979] model, but utilizes an iterative approach for computing friction factors. Dissipation rate was estimated using the relationship described in Gross et al. [1994].

Observations

The present observations were obtained during the deployment period from July 8 through September 26, 1996. On August 29, 1996, Hurricane Edouard's winds reached their maximum speed of 140 mph (category 4 on the Saffir-Simpson Hurricane Scale), and the translational speed peaked at 1000 km d^{-1} approximately 700 km south of the mooring site (Fig. 1). Hurricane Edouard maintained category 4 status for approximately seven days. Hurricane Hortense reached category 4 status on September 13, 1996, roughly 800 km south of the mooring site, but decreased in intensity to category 3 on the same day. At that point, winds were 120 mph, and the translational speed was 1500 km d^{-1}. The eye of Hurricane Edouard passed within about 110 km of the mooring on September 2, 1996 and the eye of Hurricane Hortense passed within 350 km of the on September 14, 1996. The physical and optical effects of the passages of Hurricane Edouard and Hurricane Hortense are illustrated in the time series shown in Fig. 2.

Wind speed (10 m above the surface) did not exceed 10 m s^{-1} until the passage of Hurricane Edouard when winds peaked at 28 m s^{-1} (Fig. 2a). The water column was highly stratified before the passage of Edouard as indicated by the temperature time series shown in Fig. 2b. The mixed-layer depth (MLD; computed using a 1° temperature difference criterion) deepened from 12 m to a depth of 67 m shortly after the passage of Edouard (Fig. 2b). The general mixing effect of the hurricane led to entrainment of cool, deeper waters into the upper layer and to mixing of upper layer warm waters with cooler, deeper waters. The warming of deeper waters (see 68 m record) continued for about 10 days when cooling began again.

The physical effects of Hurricane Hortense at the mooring site are less obvious than those associated with Edouard because of the much greater distance between the eye of Hortense and the site, and possibly because of the greater translational speed of Hortense. Winds associated with Hurricane Hortense were more sporadic at the mooring site, occasionally exceeding 10-15 m s^{-1} from September 14 through September 19, 1996. Hortense resulted in further mixing of the water column with the MLD increasing from 18 m to near 50 m. The passage of Hortense is more evident in the sediment resuspension event (seen in optical time series) than in the physical record.

The time series of beam attenuation coefficient at 676 nm (hereafter beam c) collected with the ac-9 on BIOPS packages at 37, 52, and 68 m depths are illustrated in Figs. 2c, d, and e (note differences in ordinate scales for the three panels). This wavelength was selected for beam c because of its covariance with suspended particulate matter and its minimal absorption due to dissolved humic acids. Sediment resuspension caused by

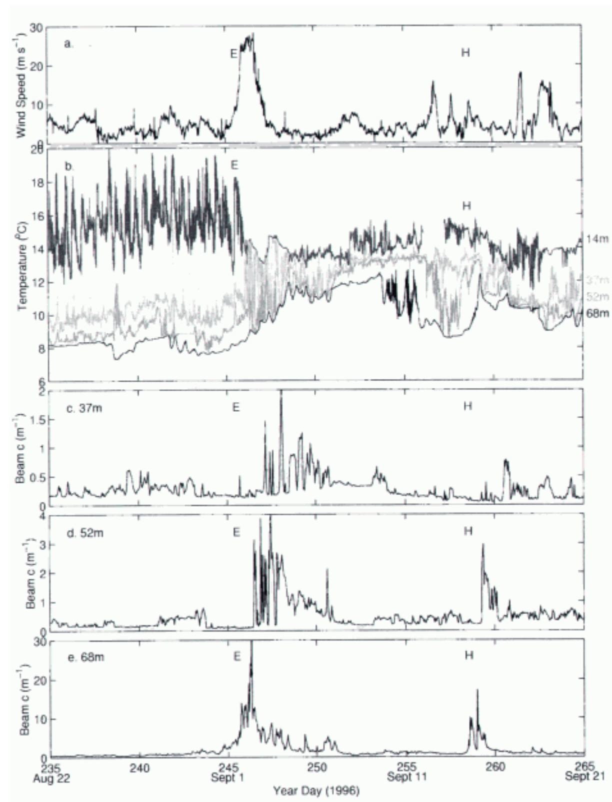

Figure 2. a. Time series of wind speed. Passages of Hurricane Edouard (E) and Hurricane Hortense (H) are indicated. b. Time series of temperature (sampling interval is 7.5 min) collected at 14, 37, 52, and 68 m depths. c. Time series of hourly average beam attenuation coefficient (676 nm) at 37 m depth. d. Same as c. for 52 m depth. e. Same as c. for 68 m depth. Note differences in ordinate scales between c, d, and e.

Hurricane Edouard first became evident in the beam c record when the storm was greater than 900 km from the CMO site. The greatest beam c values (up to about 30 m^{-1}) are seen in the near bottom (68 m) time series during the time of closest passage, however the signal is clearly seen in the 37 m depth record (up to 2 m^{-1}) as well. The beam c values are reduced by about a factor of five between 68 and 52 m and by about a factor of two between 52 and 37 m. The NDBC buoy shows that the significant wave height exceeded 9 m at this time. It is worth noting that the onset of the increased beam c values occurred first at 68 m, then about a half-day later at 52 m, and finally an additional half-day later at 37 m (Fig. 2). The return of beam c values to pre-hurricane levels was slower at the shallower depths than at the deeper depths. This is consistent with size distributions biased toward smaller particles (with lower settling velocities) at the shallower depths.

Figure 3 shows curves for size distributions taken six hours apart, beginning 12 hours before the peak in Hurricane Edouard-induced bottom pressure. The volume distributions clearly indicate the presence, disappearance, and reestablishment of large particles in the water column as the intensity of the hurricane-induced bottom currents and oscillations increased to their maximum and then weakened as the hurricane moved away from the bottom tripod. These data support the photographic results that show high levels of localized shear and turbulence (e.g., turbulent dissipation rate) in the water column, due to currents and waves, broke up flocculates. These flocs then rapidly reappeared as the intensity of turbulence weakened.

The greatest increases in beam c did not coincide with the time of closest passage of Hortense. At the time of closest passage, winds peaked at 11 m s^{-1} and significant wave height was 4 m at the NDBC buoy site. The cause(s) for the abrupt dip and then rise in the beam c record at 68 m (Fig. 2e), is not obvious. One hypothesis is that the sediments could have been resuspended some distance away from the site and then advected past the mooring. This possibility seems unlikely in that the increase in beam c did not occur at all depths at the same time. The signal was first observed at the bottom, then about three-fourths of a day later at 52 m, and then an additional three-fourths of a day later at 37 m. It is possible that two trains of wind-generated surface waves could have caused the successive peaks.

The principle physical process that determines the structure of the near-bottom flow field on a continental shelf is the interaction of surface waves with mean currents [Glenn and Grant, 1987].

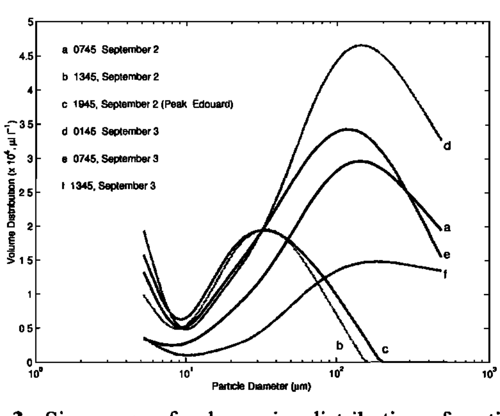

Figure 3. Six curves of volume size distribution of particles (µl l^{-1}) at six hour intervals, beginning 12 hours prior to the peak of Hurricane Edouard-induced bottom rms pressure (1945 on September 2).

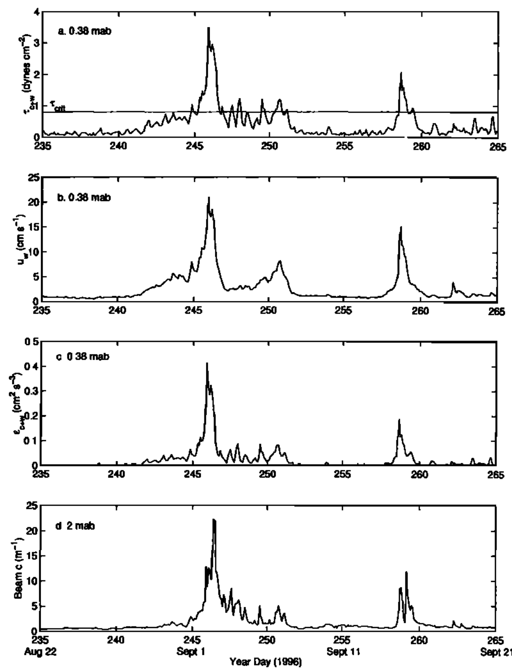

Figure 4. a. Time series of current-wave bottom shear stress at 0.38 mab computed using near-bottom current measurements (half-hour averages), wave orbital velocity, and the model presented in Christoffersen and Jonsson (1985). b. Time series of wave-orbital velocity at 0.38 mab. c. Time series of dissipation rate at 0.38 mab calculated using friction velocity derived from the Christoffersen and Jonsson (1985) model. d. Beam attenuation coefficient (676 nm) at 68 m (2 mab).

The current-wave interaction has been shown to be a non-linear phenomenon (e.g., Grant and Madsen [1979]; Christoffersen and Jonsson [1985]; Glenn and Grant [1987]). The frequency differences between waves and mean currents result in an oscillatory wave boundary layer within a relatively steady current boundary layer. The small scale of the wave boundary layer causes the wave boundary shear stress to be an order of magnitude greater than that of the shear stress associated with a current of comparable magnitude. The suspension of sediment by waves in the absence of strong, subcritical currents is not unexpected (e.g., Grant and Madsen [1979]; Glenn and Grant [1987]); it is associated with the time-varying part of shear stress, which has oscillatory amplitudes clearly in excess of critical values. To characterize the near-bottom flow field, combined current-wave shear stresses must be considered.

Sediment is expected to be resuspended when bottom shear stresses exceed a "critical" shear stress [Twichell et al, 1987]. The critical combined current-wave shear stress was first exceeded at the time of increased sediment resuspension during the passage of Hurricane Edouard (Fig. 4a). Current-wave shear stress values periodically exceeded the critical value (up to a maximum of about 3.5 dynes cm^{-2} during the time of greatest sediment resuspension) for about five days following the peak of the Hurricane Edouard winds. Mean current shear stress exceeded the critical value during the passage of Edouard as well, with τ_c exceeding 2.5 dynes cm^{-2} (data not shown). Sediment resuspension associated with Edouard was possibly due to intense bottom mean currents with little interaction with waves. In contrast, the sediment resuspension caused by Hurricane Hortense occurred when boundary shear stresses associated with currents were below critical values and current-wave shear stresses were high. The current-wave bottom shear stress reached 2 dynes cm^{-2}.

Hurricane Edouard resulted in a ten-fold increase in wave-orbital velocity (u_w) at a depth of 0.38 mab (Fig. 4b); u_w increased from approximately 2 to 15 cm s^{-1} with the passage of Hurricane Hortense. Hurricane Edouard resulted in values of dissipation rate (ε_{c+w}, at 0.38 mab) increasing 20-fold (Fig. 4c). Dissipation rates following the passage of Hurricane Hortense also increased by a factor of 20. For both hurricanes, peaks in ε_{c+w} and u_w coincided with the highest sediment resuspension seen in the beam c records (Fig. 4).

Regression analysis between mean current bottom shear stress (0.38 mab) and beam c (68 m depth) resulted in a correlation of 0.68 over the period of passage of Hurricane Edouard (August 22 through September 11, 1996). The correlation between τ_c (0.38 mab) and beam c (68 m depth) for the period of Hurricane Hortense (September 11 through September 21, 1996) was 0.007. Regression analysis performed for combined current-wave bottom shear stress (0.38 mab) and beam c (68 m) over the period of passage of Edouard gave a correlation of 0.80. A correlation of 0.75 was found between τ_{c+w} (0.38 mab) and beam c (68 m) during the passage of Hurricane Hortense. These analyses suggest that the sediment resuspension associated with Hurricane Edouard was primarily forced by currents with lesser interaction with waves. In contrast, Hurricane Hortense sediment resuspension was likely dominated by wave interaction with little influence from mean currents.

Summary

The present comprehensive physical and optical measurements have captured the impacts of two closely spaced hurricanes. The sediment resuspension associated with Hurricane Edouard was primarily locally driven through near-bottom current processes with secondary influence from waves. In contrast, Hurricane Hortense passed much further from the site, and caused sediment resuspension through remote forcing via near-bottom wave processes (i.e., surface gravity waves generated some distance away) with comparatively little interaction with mean currents. Evidence for this can be found in the correlation between mean current bottom shear stress and beam c, and between combined current-wave bottom shear stress and beam c. Our measurements show that particles were suspended more than 30 m above the ocean bottom during both hurricanes. Volume size distributions were biased towards small particles due to flocculate disaggregation during the peak of Hurricane Edouard. Throughout the periods of Hurricanes Edouard and Hortense, sediment resuspension occurred in accordance with the critical shear stress criterion for combined wave and current shear stress.

Acknowledgments. This work was supported by the Office of Naval Research as part of the Coastal Mixing and Optics program We would also like to thank John Trowbridge, Steve Lentz, Joe McNeil and Zenitha Chroneer for their assistance with data analysis and development of the manuscript; David Porter and Donald Thompson for their satellite images and analyses; Murray Levine who shared the mooring platform with us; and Derek Manov, David Sigurdson, Erin Lutrick, and Chuck Pottsmith for their engineering and technical support.

References

Agrawal, Y. C., and H. C. Pottsmith, Laser diffraction particle sizing in STRESS, *Cont. Shelf Res.*, *14*, 1101-1121, 1994.

Biscaye, P. E., R. F. Anderson, and B. L. Deck, Fluxes of particles and constituents to the eastern United States continental slope and rise: SEEP I, *Cont. Shelf Res.*, *8*, 855-904, 1988.

Cacchione, D. A., and D. E Drake, Shelf sediment transport, in *The Sea*, *9*, edited by B. LeMehaute and D.M. Hanes, pp. 729-774, John Wiley, New York, NY, 1990.

Chang, G. C., T. D. Dickey, D. V. Manov, D. E. Sigurdson, and J. D. McNeil, Data report: Coastal Mixing and Optics deployment I, *OPL-4-97*, Ocean Physics Laboratory, University of California, Santa Barbara, CA 1997.

Christoffersen, J. B., and I. G. Jonsson, Bed friction and dissipation in a combined current and wave motion, *Ocean Eng.*, *12*, 387-423, 1985.

Churchill, J. H., The effect of commercial trawling on sediment resuspension and transport over the Middle Atlantic Bight continental shelf, *Cont Shelf Res.*, *9*, 841-864, 1989.

Dickey, T., D. Frye, H. Jannasch, E. Boyle, D. Manov, D. Sigurdson, J. McNeil, M. Stramska, A. Michaels, N. Nelson, D. Siegel, G. Chang, J. Wu, and A. Knap, Initial results from the Bermuda Testbed Mooring program, *Deep-Sea Res.*, *45*, 771-794, 1998.

Glenn, S. M., and W. D. Grant, A suspended sediment stratification correction for combined wave and current flows, *J. Geophys. Res.*, *92*, 8244-8264, 1987.

Grant, W. D., and O. S. Madsen, Combined wave and current interaction with a rough bottom, *J. Geophys,. Res.*, *84*, 1797-1808, 1979.

Gross, T. F., A. J. Williams, and E. A. Terray, Bottom boundary layer spectral dissipation estimates in the presence of wave motions, *Cont. Shelf Res.*, *14*, 1239-1256, 1994.

Madsen, O. S., L. D. Wright, J. D. Boon, and T. A. Chisholm, Wind stress, bed roughness, and sediment suspension on the inner shelf during an extreme storm event, *Cont. Shelf Res*, *13*, 1303-1324, 1993.

Nittrouer, C. A., and L. D. Wright, Transport of particles across continental shelves, *Rev. of Geophys.*, *32*, 85-113, 1994.

Nowell, A. R. M., Effects of biological activity on the entrainment of marine sediments, *Mar. Geol.*, *42*, 133-153, 1983.

Tennekes, H., and J. L. Lumley, *A First Course in Turbulence*, 300 pp., The MIT Press, Cambridge, MA, 1972.

Trowbridge, J. H, and O. S. Madsen, Turbulent wave boundary layers, 1, Model formulation and first-order solution, *J. Geophys. Res.*, *89*, 7989-7997, 1984.

Twichell, D. C., B. Butman, and R. S. Lewis, Shallow structure, surficial geology, and the processes currently shaping the bank, in *Georges Bank*, edited by R.H. Backus, pp. 31-38, MIT Press, Cambridge, MA, 1987.

Williams, A. J., 3rd, J. S. Tochko, R. L Koehler, W. D. Grant, T. F. Gross, and C. V. R. Dunn, Measurement of turbulence in the oceanic bottom boundary layer with an acoustic current meter array, *J. Atmos. and Ocean Tech.*, *4*, 312-327, 1987.

Y. C. Agrawal, Sequoia Scientific, Inc., P. O Box 592, Mercer Island, WA 98040 (e-mail: yogi@sequoiasci.com)

G. C. Chang and T. D. Dickey, Ocean Physics Laboratory, University of California at Santa Barbara, 6487 Calle Real Unit A, Goleta, CA 93117 (e-mail: grace@icess.ucsb.edu; tommy@icess.ucsb.edu)

P. S. Hill, Department of Oceanography, Dalhousie University, Halifax, Nova Scotia, Canada B3H 4J1 (e-mail: phill@phys.ocean.dal.ca)

A. J. Williams, 3rd, Bigelow 110 – ms 12, AOP&E, Woods Hole Oceanographic Institution, 98 Water Street, Woods Hole, MA 02543 (e-mail: awilliams@whoi.edu)

(Received April 6, 1998; revised July 30, 1998;
accepted August 7, 1998)